



## ToF-SIMS cluster ion imaging of hippocampal CA1 pyramidal rat neurons

J.T. Francis<sup>a,\*</sup>, H.-Y. Nie<sup>a</sup>, A.R. Taylor<sup>b</sup>, M.J. Walzak<sup>a</sup>, W.H. Chang<sup>a</sup>, D.F. MacFabe<sup>b</sup>, W.M. Lau<sup>a</sup>

<sup>a</sup> Surface Science Western, Room G-1, WSC, The University of Western Ontario, London, Ontario N6A 5B7 Canada

<sup>b</sup> The Kilee Patchell-Evans Autism Research Group, Departments of Psychology and Psychiatry, Division of Developmental Disabilities, Shulich School of Medicine and Dentistry, The University of Western Ontario, Room 7252, SSC, London, Ontario N6A 5C2, Canada

### ARTICLE INFO

#### Article history:

Available online 18 May 2008

#### Keywords:

ToF-SIMS  
Cluster ion imaging  
Hippocampus  
Neuron  
Sub-cellular  
Tissue fixation  
Propionic acid  
Autism spectrum disorder

### ABSTRACT

Recent studies have demonstrated the power of time-of-flight secondary ion mass spectrometry (ToF-SIMS) cluster ion imaging to characterize biological structures, such as that of the rat central nervous system. A large number of the studies to date have been carried out on the “structural scale” imaging several mm<sup>2</sup> using mounted thin sections. In this work, we present our ToF-SIMS cluster ion imaging results on hippocampal rat brain neurons, at the cellular and sub-cellular levels. As a part of an ongoing investigation to examine gut linked metabolic factors in autism spectrum disorders using a novel rat model, we have observed a possible variation in hippocampal *Cornu ammonis* 1 (CA1) pyramidal neuron geometry in thin, paraformaldehyde fixed brain sections. However, the fixation process alters the tissue matrix such that much biochemical information appears to be lost. In an effort to preserve as much as possible this original information, we have established a protocol using unfixed thin brain sections, along with low dose, 500 eV Cs<sup>+</sup> pre-sputtering that allows imaging down to the sub-cellular scale with minimal sample preparation.

© 2008 Published by Elsevier B.V.

### 1. Introduction

Over the past few years, there has been an almost exponential increase in the number of studies that showcase the inimitable capacity of time-of-flight secondary ion mass spectrometry (ToF-SIMS) in the analysis and characterization of biological materials. Such specimens include sectioned rat and mouse brains and single cells [1–6]. Most recently, 3D images have been reconstructed from shallow image depth profiles on individual cells [7].

Prior to ToF-SIMS, it was all but impossible to efficiently obtain “fingerprintable”, molecular mass spectral information (meaning polyatomic fragments with more than two atoms) as a function of spatial distribution, especially at the submicron level. Techniques such as electrospray with MS<sup>n</sup> (where  $n = 2$  indicates tandem MS via triple quadrupole detection or  $n > 2$  with an ion trap) require sample extraction and/or homogenization, which eliminates the possibility of extracting any spatial information from the chemical constituents. MALDI-ToF provides only limited spatial distribution on a coarser scale than ToF-SIMS. Indeed, even more mature surface analytical techniques with imaging capability that provide at least some chemical information such as FTIR, Raman and to a lesser extent high resolution XPS are limited in the analysis and

characterization of biological samples by coarser spatial resolution, lower sensitivity, and possible severe sample damage. Arguably the most influential factor in facilitating the highly successful incursion of ToF-SIMS into the medical and biological fields relates directly to recent important technological advances in the instrumentation; in particular, the cluster primary ion sources (Au<sub>x</sub><sup>+</sup>, Bi<sub>x</sub><sup>y+</sup>, C<sub>60</sub><sup>+</sup>). These sources combine perhaps the two most desirable and indispensable capabilities in this regard: high spatial resolution (submicron level is not uncommon nowadays) imaging and “soft” ionization resulting in unprecedented secondary ion yields of increasingly larger mass, molecular species. Much ground-breaking work has been done with cluster ion sources by Arlinghaus, Hagenhoff, Winograd, Vickerman and others. For excellent recent reviews see for example, Johansson [8] and Brunelle [9].

Of course, with such technological advances comes the desire to clearly image smaller and smaller features such as cells (or indeed parts of cells) whilst still extracting the most (i.e. highest mass) chemical information possible. To this end, sample preparation and experimental design become paramount in achieving these goals. Many of the ToF-SIMS studies cited above were carried out on thin tissue sections, typically 10's of microns thick, prepared using well established techniques (or customized variants thereof). These have been employed for decades by researchers in the biological/medical field. The goal is to have a UHV compatible sample with minimal topography, that also reflects the initial

\* Corresponding author.

E-mail address: [jfranci2@uwo.ca](mailto:jfranci2@uwo.ca) (J.T. Francis).

biochemical conditions in the living tissue or cell as closely as possible; a veritable “snapshot” of life in cross-section as it were.

Much previous work involving individual cell imaging used cultured cells, and oftentimes the selection of cells was based upon a favourably large size ( $>50\ \mu\text{m}$ ). In this work, we used  $\text{Bi}_3^+$  primary ions, following a short 500 eV  $\text{Cs}^+$  pre-sputter treatment ( $\sim 5\text{e} + 14\ \text{ions}/\text{cm}^2$ ), to image sub-cellular features in rat *Cornu ammonis 1* (CA1) hippocampus pyramidal neurons, which are typically only  $\sim 20\ \mu\text{m}$  in size, in the surrounding neuropil. The increase in overall negative secondary ion yield and improved image quality appeared to effectively outweigh the effects of a low energy  $\text{Cs}^+$  ion dose. These samples were part of an ongoing study using rats as a model investigating propionic acid, a dietary and enteric bacterial short chain fatty acid, as a possible environmental trigger for autism spectrum disorders. ToF-SIMS was thought to be an ideal tool to examine propionic acid's widespread effects on gene expression, lipid metabolism, cytoskeletal regulation and immune function [10,11]. The additional effects of paraformaldehyde tissue fixation as part of the initial sample preparation on the ability to spatially resolve sub-cellular features in neurons are explored. The fixation process arrests autolysis and putrefaction as well as coagulates soluble and structural proteins by aldehyde crosslinking [12]. This results in reduced topography for subsequent microscopic investigation. Xia and Castner [13] have used fixation processes to preserve the structure of adsorbed protein films for ToF-SIMS analysis. Finally, the extent to which chemical information is lost due to the particular fixation process is addressed.

## 2. Materials and methods

From continuing studies [10,11], adult Long Evans rats were intraventricularly infused with propionic acid (0.4  $\mu\text{l}$  of a 0.26 M solution) or 0.1 M phosphate buffered saline vehicle (pH 7.5), twice daily for 7 days through chronically implanted indwelling cannulae. Rats were sacrificed by decapitation, and brains were removed and immediately frozen at  $-70\ ^\circ\text{C}$  with OCT-embedding. Thin coronal dorsal hippocampal sections were cut on a microtome (Leica

RM2125) from the OCT-embedded brains in a cryostat operated at  $-20\ ^\circ\text{C}$ . The thin sectioned brain films with a thickness of  $\sim 30\ \mu\text{m}$  were placed on positively charged glass slides. Unfixed samples had no further treatment and were introduced into the instrument in the frozen state. The fixed samples were prepared using standard methods by transcardiac perfusion/postfixation with ice cold 4% paraformaldehyde in 0.1 M phosphate buffered saline under deep sodium pentobarbital anaesthesia [10]. All ToF-SIMS analyses were performed at ambient temperature. All animal procedures were in accordance with guidelines of the Canadian Council on Animal Care and approved by the University of Western Ontario Animal Use Committee.

An ION-ToF (Gmbh) ToF-SIMS IV equipped with a Bi liquid metal ion source was employed in this study. The primary analysis beam was 25 keV  $\text{Bi}_3^+$  operated in the Burst Alignment mode [14] with a 10 kHz repetition rate and a pulse width of 100 ns. The target current was  $<0.2\ \text{pA}$  and the spot size was estimated to be  $\sim 300\ \text{nm}$ . Mass analysis was performed via a single stage reflectron ToF analyzer, at 2 V with 10 keV post acceleration. A pulsed, low energy (18 eV) electron flood was employed to neutralize sample charging; the current was maintained below  $\sim 20\ \mu\text{A}$  maximum to avoid sample damage. A second 500 eV  $\text{Cs}^+$  beam, with 1 nA primary current and a raster size of  $500\ \mu\text{m} \times 500\ \mu\text{m}$  was used to pre-sputter areas of interest prior to  $\text{Bi}_3^+$  imaging.

## 3. Results and discussion

Fig. 1 depicts selected negative secondary ion images acquired from the pyramidal layer of the CA1 hippocampus on an unfixed tissue sample. A 30 s,  $\text{Cs}^+$  pre-sputter was applied prior to  $\text{Bi}_3^+$  imaging. The  $\text{C}_x\text{H}_y^-$  image is a sum of several images, with  $x = 1-3$  and  $y = 0, 1$ . The image denoted as  $m/z\ 185$  is tentatively assigned to  $\text{C}_{12}\text{H}_{25}\text{O}^-$ .

The structure imaged appears to be a pyramidal neuron in cross-section. More specifically, the size of the roughly round structure delineated especially in the CN- image is consistent with a neuronal soma structure ( $\sim 20-30\ \mu\text{m}$ ). The prominent, void-

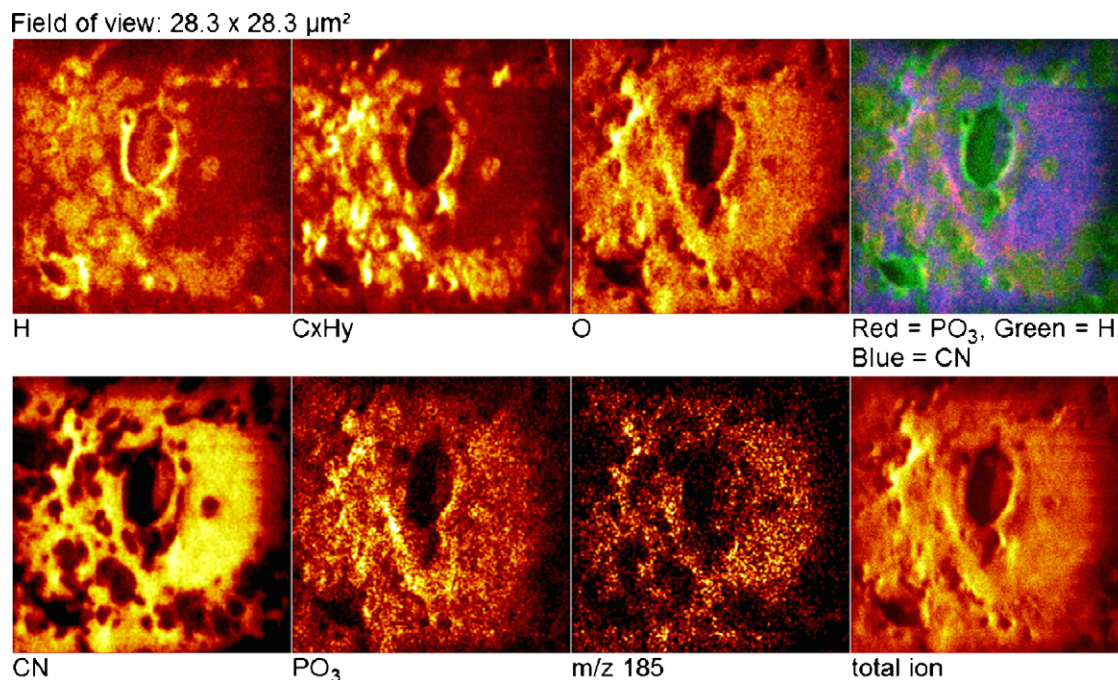


Fig. 1. Negative secondary ions images of CA1 hippocampal neuron in unfixed tissue, following 30 s, 500 eV  $\text{Cs}^+$  pre-sputter.

like, oval-shaped feature in the central portion of the images could thus correspond to the cell nucleus; its size is again consistent with such an assignment. The kidney-shaped structure to the right of the void, which displays prominent  $\text{CN}^-$ ,  $\text{O}^-$  and  $m/z$  185 intensities with concomitant lower  $\text{H}^-$  and  $\text{C}_x\text{H}_y$  may be evidence

of another organelle, possibly the rough endoplasmic reticulum. The enhanced  $\text{CN}^-$  intensity, perhaps indicative of a localization of proteins and nucleic acids, agrees with the function of this organelle in protein translation and transport between the nucleus and the cellular membrane. The  $\text{H}^-$  image is particularly rich in

Field of view:  $20.5 \times 20.5 \mu\text{m}^2$

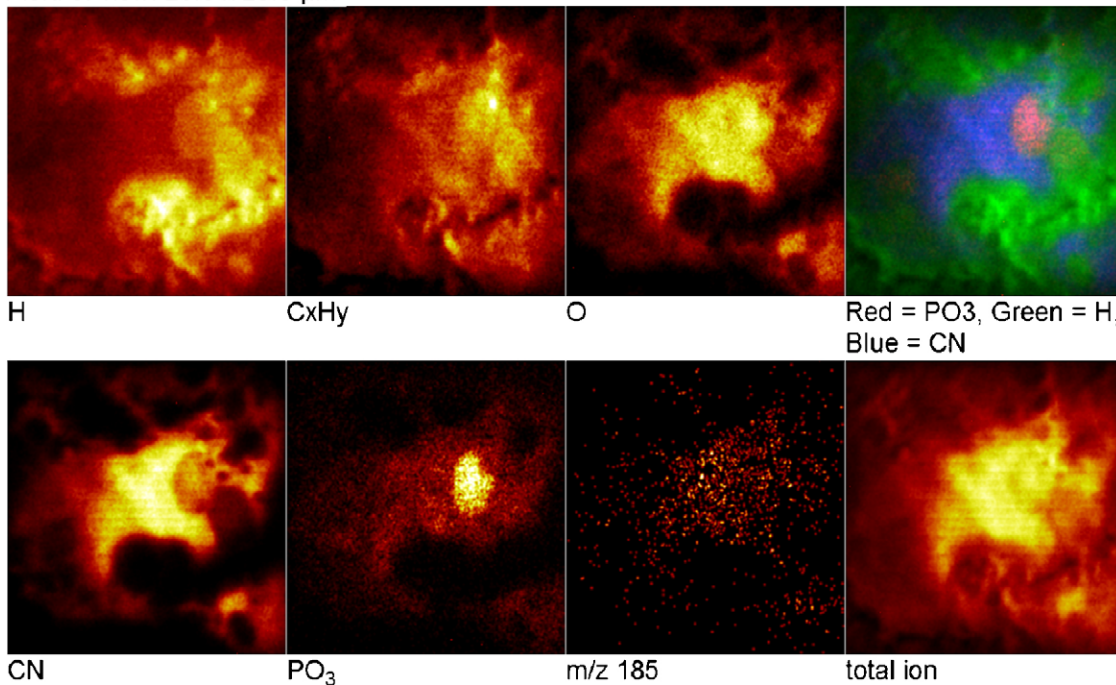


Fig. 2. Negative secondary ions images of second CA1 hippocampal neuron in unfixed tissue, following 30 s, 500 eV  $\text{Cs}^+$  pre-sputter.

Field of view:  $15.6 \times 15.6 \mu\text{m}^2$

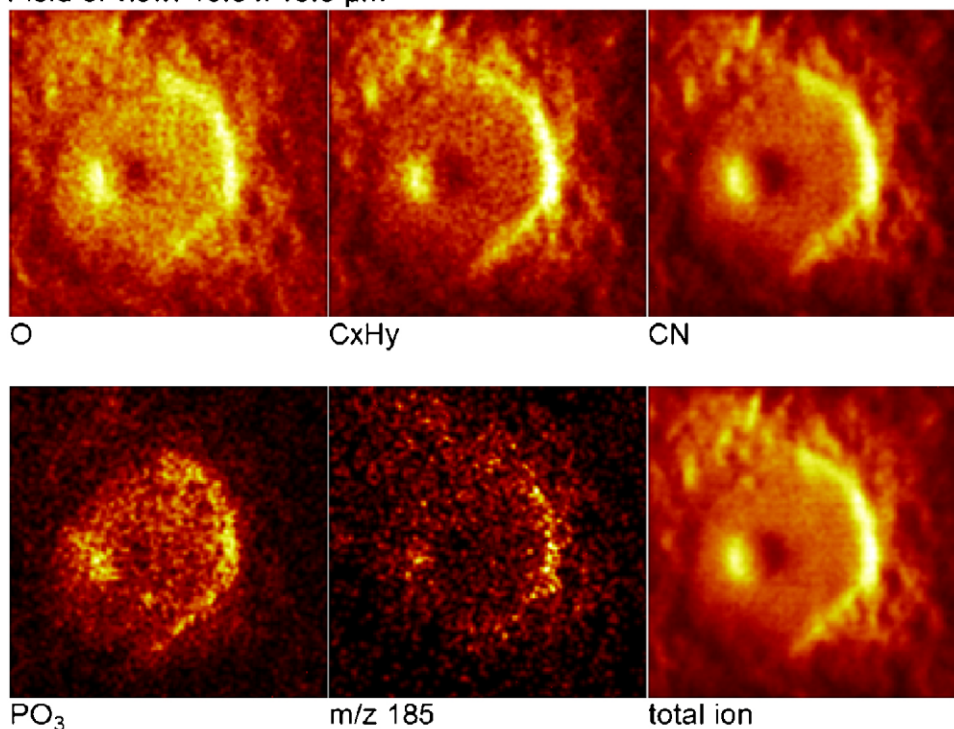


Fig. 3. Negative secondary ions images of CA1 hippocampal neuron in fixed tissue, following 30 s, 500 eV  $\text{Cs}^+$  pre-sputter.

minute detail and may reflect various structural entities within the cell cytoplasm. Interestingly, this image has a peculiar enhanced intensity that vividly outlines the void-like feature in the center potentially ascribed to the nucleus. It could be imagined that this arises from the fibrous cytoskeletal proteins that make up the inner nuclear membrane. Fig. 2 depicts a second area imaged on the same unfixed tissue sample used for Fig. 1. Again, it appears that a pyramidal neuronal soma structure has been captured in cross-section. Although not as sharp as the image in Fig. 1, possibly due to local topographical variations in the thin tissue section, many of the observations and possible assignments made for the cell in Fig. 1 also apply in this case. However, there is one important extra detail in these ion images, as evidenced by the egg-shaped feature at the right of the images. This feature is also particularly well defined by the  $\text{PO}_3^-$  image, and it is accompanied by a kidney-shaped structure as defined in the  $\text{CN}^-$  image, to the left of it. Based upon these observations, one could argue that this is the cell nucleus, with the  $\text{PO}_3^-$  being at least partly due to the presence of DNA/RNA and the  $\text{CN}^-$  defining the rough endoplasmic reticulum next to it.

It must be noted that in imaging the two hippocampal CA1 features in the unfixed tissue sample, it was very difficult to locate the pyramidal neurons in the as-received condition. Only after the 30 s, 500 eV  $\text{Cs}^+$  pre-sputter treatment did the neuronal soma become readily apparent. Although this technically means an ion dose exceeding the static limit has been applied even before  $\text{Bi}_3^+$  imaging has begun, the negative secondary ion yield enhancement appears to outweigh the possible loss of some intact, large molecular weight, chemical information.

Negative secondary ion images acquired from a fixed tissue thin section using the same methodology as in Figs. 1 and 2 are presented in Fig. 3. The structure appears to be consistent in size and shape with a CA1 hippocampal pyramidal neuron. The circular feature to the left inside the main circular feature could be the nucleus. What is readily apparent upon comparison of Fig. 3 to Figs. 1 and 2 is the lack of fine detail, and the fact that all the ion images in Fig. 3 look similar. Only  $\text{PO}_3^-$  and perhaps  $m/z$  185 appear to be somewhat more localized within the region ascribed to the soma. Indeed, although the region possibly corresponding to the cytoplasm is quite flat, as is the surrounding matter, the soma appears to be depressed in to the surface plane, with the nucleus slightly proud. This results in what appears to be a relatively uninformative set of images from a chemical standpoint, with shadowing from the slightly depressed soma topography representing the major variation in secondary ion yield.

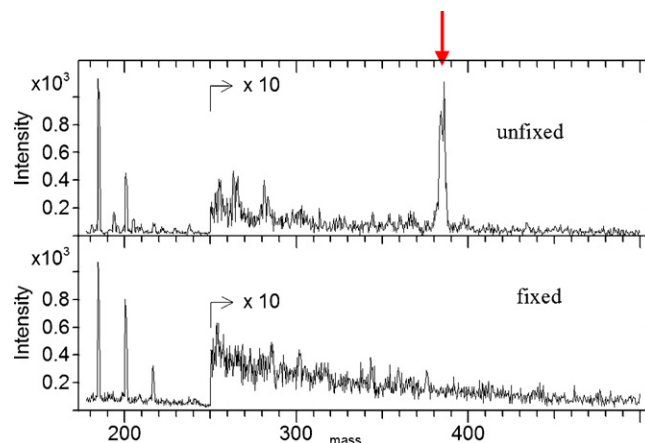


Fig. 4. Abundance of  $m/z$  385 ( $-ve$ ) in unfixed vs. fixed CA1 hippocampal neurons, following a 30 s  $\text{Cs}^+$  treatment (burst alignment spectra from raw data files).

Fig. 4 depicts the burst alignment mass spectra extracted from the raw data files for the images in Figs. 1 and 3. This illustrates a deleterious effect of the fixation process, in that important components of interest, such as cholesterol in this case, can be “stripped” out prior to imaging. It also illustrates that larger species such as the cholesterol-derived fragment at  $m/z$  385 are not totally obliterated by the 500 eV  $\text{Cs}^+$  pre-treatment.

Fig. 5 shows a comparison of brain tissue of rats that received intraventricular propionic acid infusions, a novel model of autism spectrum disorders [10,11], to PBS vehicle infused rat controls. The images are pyramidal neurons in the CA1 hippocampal region, in paraformaldehyde fixed tissue. Based upon our previous experience with fixed tissue, as presented in Fig. 3, we found  $\text{PO}_3^-$  was the most diagnostic species yielding the best contrast. These images may reflect  $\text{PO}_3^-$  groups on nuclear DNA or cytoplasmic cytoskeletal structural proteins, such as neurofilaments. The two brains exhibit clearly different cell morphology, with the propionic acid autism model rat possessing relatively smaller, more irregularly shaped, CA1 pyramidal neuronal cells. Although these results are extremely preliminary, this is consistent with the known effects of propionic acid on neurofilament expression and phosphorylation, which play a major role in neuronal structural integrity [15–17] and the smaller, increased packing density of neurons in autism. [10]. Further studies are underway examining these imaging results with traditional light and electron microscopic techniques in the same tissue.

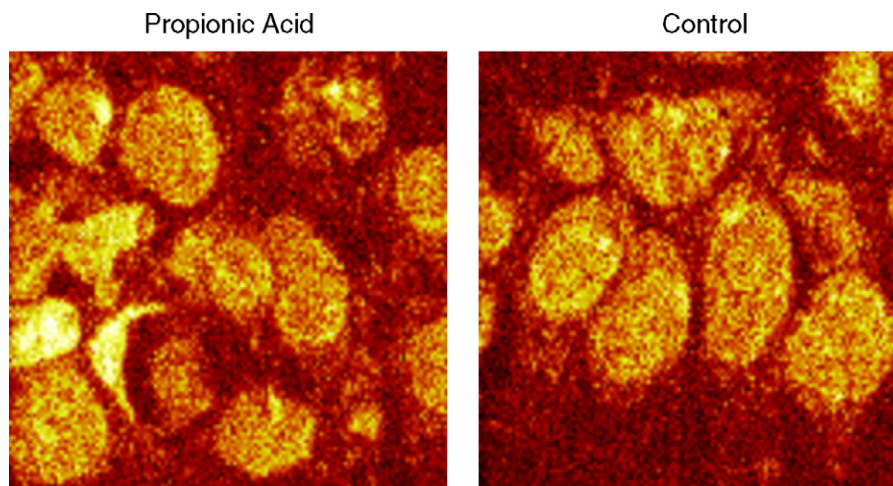


Fig. 5. Comparison of CA1 hippocampal neuron morphology between propionic acid treated rats and PBS vehicle controls.  $\text{PO}_3^-$  images on fixed tissues,  $50 \mu\text{m} \times 50 \mu\text{m}$  area.

#### 4. Conclusions

In this work,  $\text{Bi}_3^+$  primary ion imaging, following a short 500 eV  $\text{Cs}^+$  pre-sputter treatment, was used to resolve sub-cellular features in rat brain *C. ammonis* 1 hippocampal neurons, which are typically only  $\sim 20 \mu\text{m}$  in size, in their unfixed surrounding neuropil. The increase in overall negative secondary ion yield and improved image quality appeared to effectively outweigh the effects of a low energy  $\text{Cs}^+$  ion dose that technically exceeds the static limit. Tentative assignments to the cellular structures were made based on the chemical information provided by ToF-SIMS images. Tissue fixation effects appear deleterious in this particular work as important components can be stripped out of the tissue and cells; including cholesterol and other lipids, which are affected in many propionic acid dependant events and also autism spectrum disorders. In addition, the resulting topographical changes potentially serve to diminish image quality instead of improving it. Nonetheless, ToF-SIMS analysis of both fixed and unfixed tissue does show promise as a useful tool to examine animal models of neurometabolic disorders, including autism.

#### References

- [1] A. Benninghoven, *Angew. Chem. Int. Ed. Engl.* 33 (1994) 1023.
- [2] D. Léonard, H.J. Mathieu, J. Fresenius, *Anal. Chem.* 365 (1999) 3.
- [3] A.M. Belu, D.J. Graham, D.G. Castner, *Biomaterials* 24 (2003) 3635.
- [4] P. Sjövall, J. Lausmaa, B. Johnsson, *Anal. Chem.* 76 (2004) 4271.
- [5] K.R. Amaya, E.B. Monroe, J.V. Sweedler, D.F. Clayton, *Int. J. Mass Spectrom.* 260 (2007) 121.
- [6] H. Nygren, B. Hagenhoff, P. Malmberg, M. Nilsson, K. Richter, *Microsc. Res. Tech.* 70 (2007) 969–974.
- [7] S.G. Ostrowski, M.E. Kurczy, T.P. Roddy, N. Winograd, A.G. Ewing, *Anal. Chem.* 79 (2007) 3554.
- [8] B. Johansson, *Surf. Interface Anal.* 206 (2006) 1401.
- [9] A. Brunelle, D. Touboul, O. Laprevote, *J. Mass Spectrom.* 40 (2005) 985.
- [10] D.F. MacFabe, D.P. Cain, K. Rodriguez-Capote, A.E. Franklin, J.E. Hoffman, F. Boon, A.R. Taylor, M. Kavaliers, K.-P. Ossenkopp, *Behav. Brain Res.* 176 (2007) 149.
- [11] D.F. MacFabe, K. Rodríguez-Capote, J.E. Hoffman, A.E. Franklin, Y. Mohammad-Asef, A.R. Taylor, F. Boon, D.P. Cain, M. Kavaliers, F. Possmayer, K.-P. Ossenkopp, *Am. J. Biochem. Biotechnol.* 4 (2008) 146.
- [12] W.-S. Chu, B. Furusato, K. Wong, I.A. Sesterhenn, F.K. Mostofi, M.Q. Wei, Z. Zhu, S.L. Abbondanzo, Q. Liang, *Mod. Pathol.* 18 (2005) 850.
- [13] N. Xia, D.G. Castner, *J. Biomed. Mater. Res. Part A* 67A (2003) 179.
- [14] R.N. Sodhi, *Analyst* 129 (2004) 483.
- [15] L. Vivian, et al. *Neurochem. Res.* 27 (2002) 1691.
- [16] L.M. de Almeida, et al. *Metab. Brain Dis.* 18 (2003) 207.
- [17] A. de Mattos-Dutra, et al. *Neurochem. Int.* 33 (1998) 407.